SLAC-PUB--5183

DE90 006459

NUMERICAL SIMULATION OF CROSS FIELD AMPLIFIERS*

Kenneth Eppley
Stanford Linear Accelerator Center
PO Box 4349, Stanford, California, 94309

ABSTRACT

Cross field amplifiers (CFA) have been used in many applications where high power, high frequency microwaves are needed. Although these tubes have been manufactured for decades, theoretical analysis of their properties is not as highly developed as for other microwave devices such as klystrons. One feature distinguishing cross field amplifiers is that the operating current is produced by secondary emission from a cold cathode. This removes the need for a heater and enables the device to act as a switch tube, drawing no power until the rf drive is applied. However, this method of generating the current does complicate the simulation.

We are developing a simulation model of cross field amplifiers using the PIC code CONDOR. We simulate an interaction region, one travelling wavelength long, with periodic boundary conditions. An electric field with the appropriate phase velocity is imposed on the upper boundary of the problem. Evaluation of the integral of $E \cdot J$ gives the power interchanged between the wave and the beam. Given the impedance of the structure, we then calculate the change in the travelling wave field. Thus we simulate the growth of the wave through the device.

The main advance of our model over previous CFA simulations is the realistic tracking of absorbtion and secondary emission. The code uses experimental curves to calculate secondary production as a function of absorbed energy, with a theoretical expression for the angular dependence.

We have used this code to model the 100 MW X-band CFA under construction at SLAC, as designed by Joseph Feinstein and Terry Lee. We are examining several questions of practical interest, such as the power and spectrum of absorbed electrons, the minimum travelling wave field needed to initiate spoke formation, and the variation of output power with DC voltage, anode-cathode gap, and magnetic field.

Introduction

The crossed-field amplifier (CFA) is an outgrowth of the magnetron. Like magnetrons, it is capable of producing very high peak powers with reasonable efficiencies. Unlike magnetrons, the CFA is a true amplifier; however, it is difficult to obtain both high gain and low noise operation. In the CFA, electrons drift in the crossed electric field between anode and cathode and an external transverse magnetic field. A periodic

* Work supported by the US Department of Energy, contract DE – AC03 -- 76SF00515.

Contributed to the Conference on Computer Codes and the Linear Accelerator Community, Los Alamos, New Mexico, January 22-25, 1990

structure on the anodes supports a travelling wave whose phase velocity is designed to be equal to the $E \times B$ drift velocity. RF power is injected into an input cavity, setting up a travelling wave in the anode-cathode region. With proper choice of DC electric and magnetic fields, the wave bunches the beam and produces electron spokes which interact with the field to transfer energy to it.

Either forward or backward wave modes can be used. The backward wave CFA has the advantage that the beam sees the output cavity with its high fields first, and forms spokes quickly, while in the forward wave device a much longer distance is required before a stable spoke is produced. Also, the modulation of the reentrant beam has a much smaller effect in the backward wave CFA.

Simulation Model

Because CFA's are inherently 2D, non-linear devices, numerical simulation is important for accurate design. We are developing a simulation code based on the PIC code CONDOR [1] which can calculate the gain and efficiency of a CFA tube, for forward or backward wave modes, including reentrancy of the beam and secondary emission from the cathode. The main advance of our model over previous CFA simulations is the realistic tracking of absorbtion and secondary emission. The code uses experimental curves to calculate production of secondaries as a function of absorbed energy, with a theoretical term (basically $1/\cos(\theta)$) giving the angular dependence.

We simulate an interaction region, one travelling wavelength long, with periodic boundary conditions. Time in the simulation corresponds to progression in space around the circumference of the CFA. When the beam passes out one end of the simulation box and reenters the other side, this corresponds to shifting the box one wavelength forward.

An electric field with the appropriate phase velocity is imposed on the upper boundary (port) of the problem. We assume adiabatic change so that the port voltage V and phase ϕ depend only on the time t. We solve Maxwell's equations to obtain a self-consistent charge and field distribution.

Our calculation of the interaction between the beam and the wave is similar to that described by Yu, Kooyers, and Buneman [2]. Evaluation of the integral of $E \cdot J$ gives the power interchanged between the wave and the beam. From this power, and the impedance Z of the structure (where the energy is $.5V^2/Z$), we calculate the time derivative of the travelling wave:

$$dV/dt = (Z/V) \cdot P$$

$$d\phi/dt = (Z/V^2) \cdot R$$

where P is $\int (E \cdot J d^3x)$ using the E field corresponding to phase ϕ, and R is the integral using phase $\phi + \pi/2$.

For a backward wave mode, the beam enters at the high power output and proceeds to the input. In simulating the backward mode, power is extracted from the wave as

the beam progresses from output to input. We assume some output power level, and calculate what input level would be needed to produce this. Steady state is assumed, so that we can ignore the fact that the group velocity is different from the particle drift velocity.

The beam is reinjected after passing through the sever to determine the effect of starting with an initially modulated beam. Generally, successive passes will not exactly reproduce, especially in the low voltage section, due to space charge oscillations which are at a different frequency than the operating frequency. Real devices tend to average out phase variations over the third dimension, so our calculations tend to overestimate the phase jitter in the low voltage section.

Application to SLAC 100 MW CFA

We have used this code to model the 100 MW X-band CFA under construction at SLAC, designed by Joseph Feinstein and Terry Lee. We list the nominal specifications and the simulation results (for constant impedance and magnetic field, including the synchronous harmonic only):

Frequency: 11.424 GHz

Peak Power Output: 100 MW

RF Pulse Width: 400 ns

Pulse repetition rate: 360 pps

Anode Voltage: 120 kV [Simulation: 140 kV]

Anode Current: 1700 Amp [Simulation: 1200 Amp]

Efficiency ($\eta_e \cdot \eta_c$): $0.7 \cdot 0.7 = 0.5$ [Simulation: $0.74 \cdot 0.9 = 0.67$]

Gain: 20 db [Simulation: approx. 20 db]

RF Drive Power: 1 MW [Simulation: approx. 1 MW]

Emitter: Platinum cold cathode

Cathode dimensions: 5.50 cm radius by 1.65 cm high

Cathode current density: 29 A/cm^2 [Simulation: 21 A/cm^2]

Anode dimensions: 5.82 cm radius (336^o of circumference) by 1.65 cm high

Anode-Cathode gap: 3.175 mm

Number of anode resonators: 85

Average anode dissipation: 134 W/cm^2 at 400 ns [Simulation: 88 W/cm^2]

Peak anode dissipation: 4.7 MW/cm^2 [Simulation: 7 MW/cm^2 instantaneous peak]

Phase shift per section: 225 degrees

Phase velocity: $7.428 \cdot 10^7$ m/s

Synchronous voltage: 16.4 kV

DC magnetic field: 5-6 kGauss [Simulation: 6 kGauss]

We are examining several questions of practical interest, such as gain, efficiency, phase jitter, and the power and energy spectrum of intercepted electrons at various power levels.

Minimum RF Field Needed for Start-Up

The DC field gradient is below the threshhold for field emission, but a small number of electrons will be present due to quantum tunnelling. Simulations show that in the absence of drive these electrons do not produce secondaries, but RF power of a few hundred kW is sufficient to initiate secondary emission and form a hub.

Maximum RF Field Limitations

Calculations by Feinstein [3] using a model assuming Brillouin flow in the hub (rather than self-consistent space charge) indicated that for high RF fields, the cathode bombarding energy would become so large that the secondary emission ratio would go below unity. This occurs at 6 keV for platinum. (See Skowron [4]). If most of the deposited electrons are above this threshold, secondary emission will not maintain the hub current. Thus, it might be necessary to use a larger anode-cathode gap than would be optimal for maximum power. (A larger gap results in lower RF field strengths at the hub and thus lower anode current.)

This does not appear to be a problem when only the synchronous wave is included in the simulation. However, when the backward wave fundamental is also included, the conclusion changes (see below). With only the synchronous wave, the space charge oscillations in the hub contribute as much or more to secondary production as the travelling wave. With an initial space charge of about .001 of the steady state value (at our operating point), these oscillations are sufficient to initiate secondary production and formation of a hub. The mean absorbtion energy on the cathode changes from 300 eV with no travelling wave field to 700 eV (for our circuit) with 100 MW of RF power. The distribution is peaked at low energies (a few tens of eV) and falls off monotonically with energy, with the median absorbed energy being roughly half the mean value. These findings suggested that an oxide cathode (e.g., BeO) might perform better than platinum, since such cathodes have higher secondary yield and lower peak energy. Simulations verified that a BeO cathode allowed higher peak power than Pt when only the synchronous mode was included.

Initially the simulations included only the synchronous harmonic. The wavelengths of the other harmonics are, in general, not simply related to the synchronous wavelength, and would not be correctly modelled by the periodic boundary conditions in the simulation. However, for certain specific phase shifts, where the ratio between wavelengths is a simple fraction, e.g., 1/2 or 2/3, it is possible to model both fundamental and synchronous waves with a longer simulation region and still use periodic boundaries. For example, consider a fundamental wave with -120 degree phase shift per resonator. The synchronous wave is -120 + 360 = +240 degrees. One can model both harmonics using a simulation region of one fundamental wavelength (three resonator lengths). Because the

simulation covers an integral number of resonators, one can model all harmonics, either as separate terms or modelling the voltage across the vanes with RF ports. Another possibility is to use a fundamental with phase shift of -144 degrees, with a synchronous wave of +216 degrees. The fundamental wavelength is 3/2 the synchronous wavelength, and one can model these two modes in three synchronous wavelengths.

In the SLAC CFA the fundamental mode is -135 degrees, which has longer wavelength than the synchronous mode of 225 degrees. The fundamental amplitude at the anode is about the same as the synchronous wave, but at the cathode it is considerably stronger, since the decay constant is proportional to wavelength.

We have studied the effects of the fundamental mode for the combinations -120, +240 and -144, +216 degrees. At low power there is not much change from the synchronous only case except a small drop in efficiency. However, at higher power levels, the higher transverse fields at the cathode from the fundamental can increase the cathode bombardment energies above the maximum threshold for sustainable secondary emission. This cutoff occurs at a much lower RF power level than was found for the synchronous wave alone. For the present CFA design, the code predicts a maximum power level of about 40-60 MW, above which the cathode cannot sustain secondary emission.

A cutoff of secondary emisssion can also occur when only the synchronous mode is included, from a different mechanism. When the RF field exceeds a critical threshold, which depends on the DC voltage, gap width, and DC magnetic field, the spoke draws so much current that the hub is depleted and secondary emission ceases. For the initial SLAC design, the threshold for this effect is slightly above 100 MW at the operating point used in the simulations.

These mechanisms may account for the upper mode current cutoff observed experimentally in CFAs. These observations suggest the desirability of tapering the impedance lower near the output. They also suggest that a synchronous fundamental (generally requiring a forward wave) might allow higher peak power, since the harmonics then are weaker at the cathode than the synchronous wave.

Parameter Study

We have begun a parameter study to find the best operating point, by varying DC voltage, anode-cathode gap, and magnetic field. Simulations indicate that maximum RF power is produced with a DC voltage about 15 to 20% above the Hartree value, consistent with observations of actual CFA's. We are studying the effects of tapering the impedance and magnetic field profiles along the circuit to maximize the output power and minimize phase jitter. Simulations indicate that with constant magnetic field and impedance, power production from the second half of the tube is very small, because the RF falls below the minimum (about 10^7 V/m at the anode) needed to hold the spoke in place. This limits the maximum gain and contributes to phase jitter, because the reactive component of induced current can produce a large phase shift even though it adds no power to the beam. Increasing the magnetic field when the voltage falls below

this threshold brings the beam closer to the Hartree condition and increases the gain by several db in some, but not all, cases.

Tapered Impedance

A taper on impedance, highest at the input, should reduce problems with current depletion, anode heating, and breakdown at the high power end, as well as improving power production and phase stability at the low power end. In practice, large impedance variations can only be attained if the phase velocity is also varied. We modified the code to permit variable phase velocities. To keep the simulation region equal to one wavelength, the zone size had to be varied continuously, and all the quantities related to the zone size had to be recalculated on every timestep. The particle coordinates do not change, so there may be either too many or too few particles at the left and right boundaries when the mesh is altered. This does not seem to create a problem as long as the change per time step is small.

We specify the taper by giving β, the phase shift per resonator, as a function of time. Empirical measurements determined the scaling of the group velocity v_g to be proportional to $\beta^{7.5}$. From this we calculate the scaling in the impedance and attenuation, which vary as v_g^{-1}, or as $\beta^{-7.5}$. If we define the impedance with respect to the voltage across a wavelength rather than the voltage across the resonator vanes, the change in mesh size varies as β^2 so the impedance then varies as $\beta^{-5.5}$. The RF voltage must change as the impedance is varied so as to conserve energy:

$$\delta V_{rf} = V_{rf} \cdot \delta Z/(2Z)$$

For the SLAC CFA, initially designed for a β of 225 degrees, the limits on β lie approximately between 210 and 250 degrees. This allows a variation in the structure impedance by a factor of 2.7. We simulated several tapers between these limits for a backward wave CFA with a BeO cathode, with 145 kV DC, 3.2 mm anode-cathode spacing, and 6 kgauss magnetic field (synchronous mode only). The best simulation result was 300 MW output power, a gain of 18.6 db, electronic efficiency 74%, circuit efficiency 87%, net efficiency 64%. Peak anode dissipation was about 10 MW/cm^2.

Anode Dissipation

One limitation on the peak power level is due to absorbtion of power by the anode. If the anode temperature goes above its melting point during the duration of the pulse, the surface will be damaged and the lifetime of the tube will be short. The temperature rise for a copper anode is given by

$$\Delta T = .311 \cdot P \cdot \tau^{1/2}$$

where T is in degrees C, P is power absorbed in watts/cm^2, and τ is the pulse width in seconds. For copper the melting point is about 600 degrees C. For a 100 ns pulse the power must be less than 6 MW/cm^2 for ΔT to be below 600 degrees. If the anode vanes are tipped with tungsten, the temperature rise will be higher, but the melting point is also higher, and the allowed dissipation will be about 10 MW/cm^2 over 100 ns.

One disadvantage of the backward wave device, according to the simulations, is that the first spoke which forms carries about twice as much current as subsequent spokes, with correspondingly higher anode dissipation. Here again, tapering the impedance helps. With the untapered design, the dissipation reaches the limit for tungsten tipped vanes at about 100 MW, while tapering the impedance can allow powers of up to about 300 MW before melting. We are also studying whether, as McDowell found [5], proper shaping of the anode vanes may further reduce dissipation.

We are examining the spatial and temporal pattern of anode absorbtion in finer detail. The values reported in this paper as peak values of dissipation represent averages over one RF period. An examination with finer time resolution suggested that the true values might be higher in some cases by as much as a factor of two, because the deposition was not uniform over a cycle. However, this would depend also on how reproducible the current pattern was from spoke to spoke. An accurate model will require simulation of the actual vane structure (see below).

Modelling the Output End of a Backward-Wave CFA

We devised a model allowing simulation of the real vane structure, for arbitrary phase shifts. We modelled the vanes for six resonators with the SLAC design, plus a drift space at each end, and quarter-wave choke cavities in cathode and anode to prevent propagation of the wave through the drift space. The voltages on the slots were constant, with a phase shift of 135 degrees between each. The voltages on the end slots were reduced for better matching of the transverse wave. The output port in the actual device causes a reduction in voltage of similar magnitude. This simulation gives a fairly good model of the fields in the drift space and should give a good idea of the anode deposition near the output. The main error in this short model is that the beam has more modulation entering the drift space than it would in the actual device. Even so, the spokes are seen to collapse almost immediately after the last slot.

This model gave an upper limit on power due to current depletion that agreed fairly well with the two-harmonic simulations described above. At a power of 40 MW, the peak anode absorbtion was 14 MW/cm^2. This assumed that the absorbtion was over the tip of the vane only, and is probably an overestimate, since some of the current is observed to go between the vanes. We wish to redo these calculations with a finer subdivision of the vanes to get a precise determination of the area of deposition.

Forward Wave Design

We modelled a forward wave circuit where the vane width and separation were reduced so that the fundamental harmonic could be used as the synchronous wave. The other harmonics are then all weaker at the cathode, and do not significantly increase the bombardment energy. Thus it is possible to use an oxide cathode and sustain peak powers of several hundred MW. There are, of course, engineering difficulties in fabricating a circuit with smaller dimensions. There is also a potential problem because the tube passes through resonance with the π mode as the voltage rises. For a backward wave,

this mode lies at voltages above the operating point and is never encountered. If the modulator rise time is fast enough, it may be possible to avoid this mode.

We scaled a structure with a fundamental at +144 degrees phase shift. The first harmonic is at -216 degrees. In the backward wave design this would have been the synchronous mode. If one shrinks the anode structure by a constant factor in the longitudinal direction, then to first order the impedance (measured with respect to the RF amplitude rather than the slot voltage) is unchanged. The circuit attenuation increases inversely with the size reduction factor.

The simulation took the 144 degree mode as the synchronous wave, reducing the resonator spacing by 2/3 to keep the same phase velocity. Thus the DC voltage, magnetic field, and anode-cathode voltage could remain as before. The circumference was left unchanged, though this could be increased if needed for higher power.

Simulations with fixed RF voltages, including the lowest two harmonics, showed that with the synchronous fundamental the cathode bombardment energies were again of the order of several hundred eV. Thus an oxide cathode could work well. Using BeO, the peak power reached about 300 MW before current depletion occurred. The anode deposition at this level was close to the limit with tungsten coating. These limits assumed the nominal circuit impedance, and both could be increased if the impedance at the high power end were reduced. At the low power end, it was found that about 3 MW input was needed to initiate spoke formation. A simulation of the entire circuit, including reentrancy, found an output power of 280 MW from an input of 3 MW, a gain of 18.4 db. The electronic efficiency was 64% and the circuit efficiency was 78%, for a net efficiency of 50%. The peak anode absorbtion was 14 MW/cm^2.

Future Work

We wish to expand our model to allow higher space harmonics for arbitrary phase shifts. We are planning to use a comoving mesh with quasi-periodic boundaries. The Poisson solver will assume exact periodicity of the charge. The electric field extrapolation across the boundaries, however, will use the analytic form of the higher harmonics, which are not periodic in the simulation region. Thus there will be a discontinuity in the fields across the boundaries but not in their calculated finite differences. The comoving mesh will keep the spokes centered so they do not cross the discontinuity. Some charge will cross between the boundaries, but hopefully this will be small enough that it does not cause problems.

We are engaged in benchmarking our simulations against existing CFA's. We wish to develop estimates of amplitude and phase jitter based on the fluctuations in the power generation and in the pass-to-pass stability. We are also examining the effects of the shape of the vanes on the anode dissipation and efficiency. We are studying whether adding slots to the cathode to increase the synchronous field near the hub will increase the gain and improve phase stability. We are continuing to study the effects of varying gap spacing, DC voltage, and magnetic field.

References

1. *CONDOR User's Manual*, B. Aiminetti, S. Brandon, K. Dyer, J. Moura, D. Nielsen, Jr., Livermore Computing Systems Document, Lawrence Livermore National Laboratory, Livermore, California, April, 1988.
2. "Time-Dependent Computer Analysis of Electron-Wave Interaction in Crossed Fields," S. Yu, G. Kooyers, O. Buneman, *Journal of Applied Physics, 36*, 8, pp. 2550-2559, August, 1963.
3. "Planar Magnetron Theory and Applications," J. Feinstein, in *Crossed-Field Microwave Devices, Volume I*, edited by E. Okress, Academic Press, 1961.
4. "The Continuous Cathode (Emitting Sole) Crossed Field Amplifier," J. Skowron, *Proceedings of the IEEE, 61*, 3, pp. 330-356, March, 1973.
5. *CFA Design Improvement Program: Part II, Final Report, Volumes I and II*, H. McDowell, Varian Associates, Inc., Beverly, Mass., June, 1982.

Figure 1. Simulation of one (slow wave) wavelength of electron position-space distribution showing electron hub and spoke. DC plus RF field vectors are plotted at the anode. The boundary conditions are conducting on the bottom, metal with imposed travelling voltage on top, and periodic on the sides. The top picture shows a strong RF field which holds the spoke tightly, while the second shows a weaker field where the spoke undergoes tumbling.

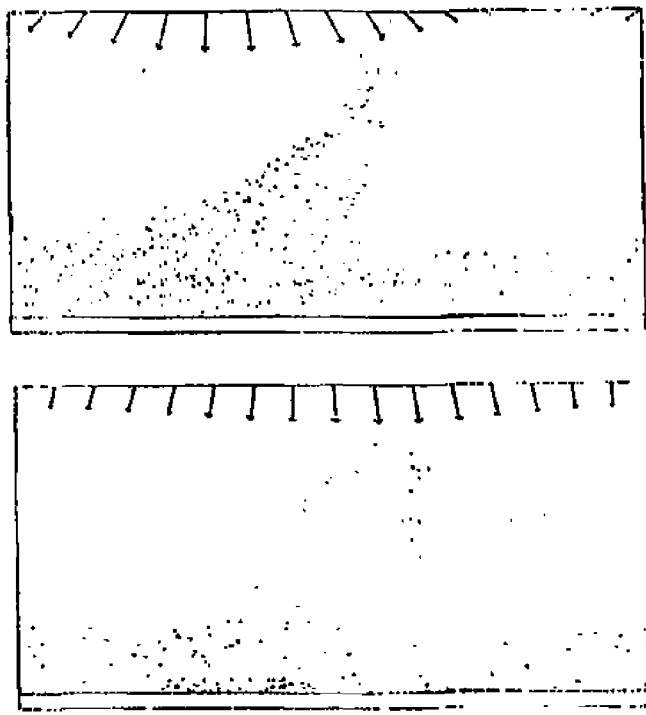

Figure 2. Schematic of a CFA showing vanes, input, output, and sever (drift space with no RF which isolates input and output).

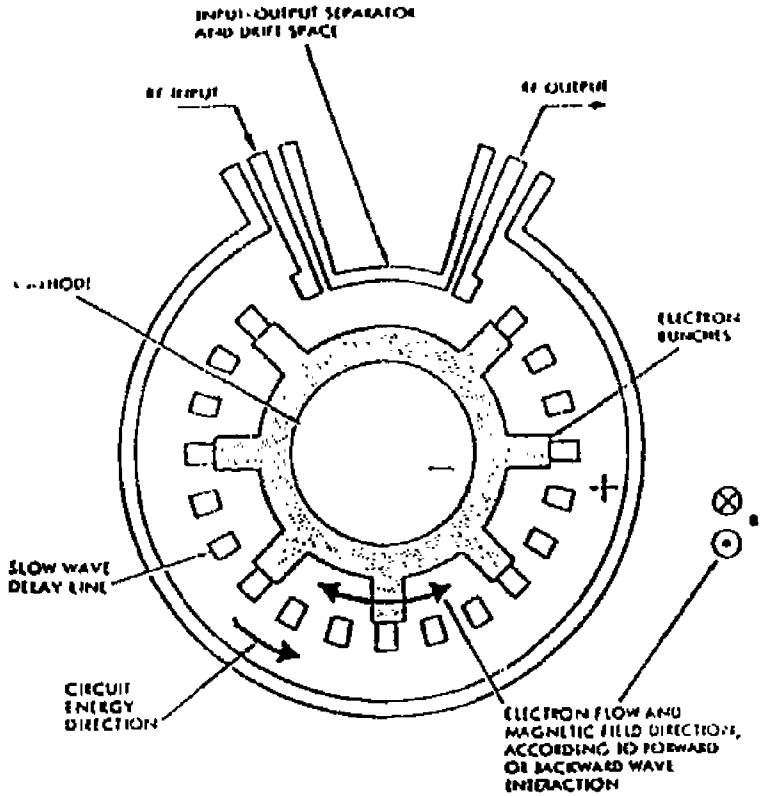

Figure 3. Onset of current depletion. Peak RF field was 77 MV/m (power level, 220 MW). DC voltage 140 kV, magnetic field 6 kGauss, anode-cathode gap .32 mm.

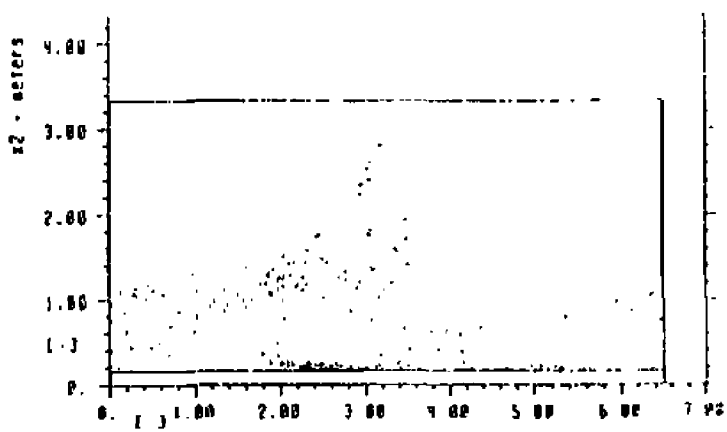

Figure 4a. Simulation of the initial SLAC CFA design, constant impedance and magnetic field. Power level (MW) versus distance (one wavelength = 6.5 mm). For a backward wave device we begin the simulation with an assumed output level and remove power from the beam to find the level that would have been needed at the input for consistency.

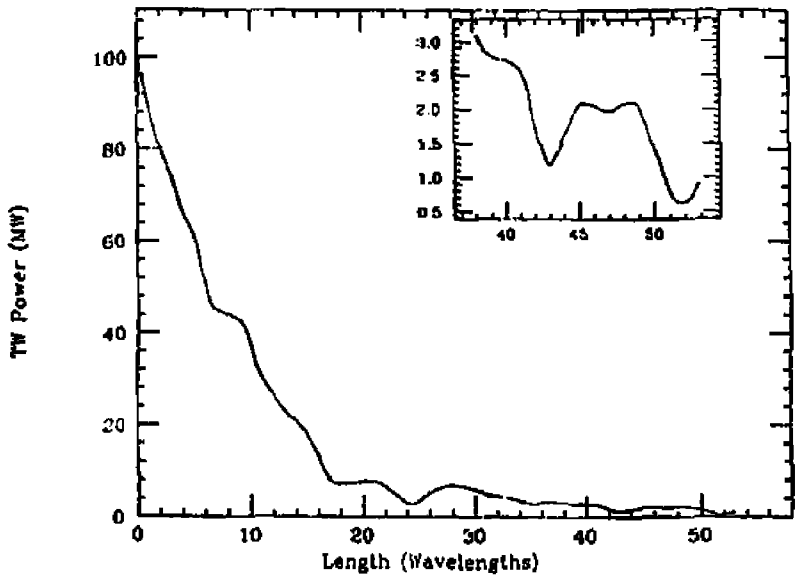

Figure 4b. Travelling wave phase versus distance.

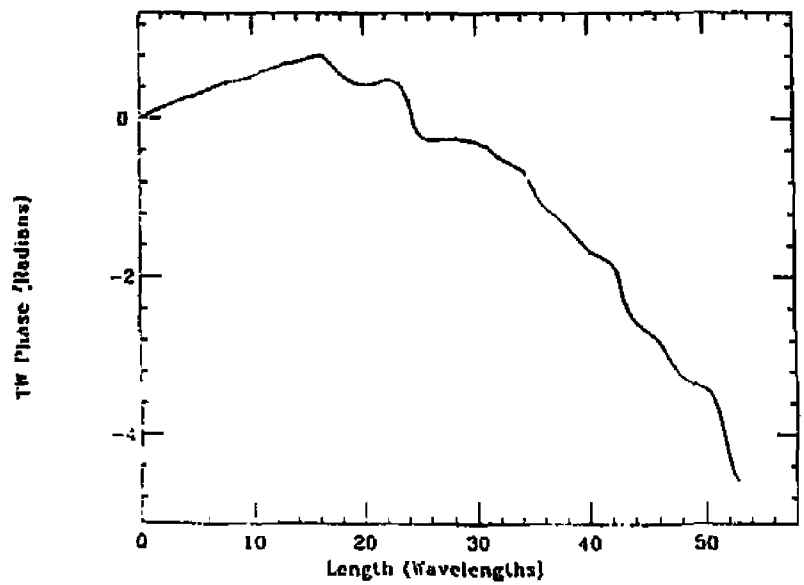

Figure 4c. Relative phase between voltage and current versus distance.

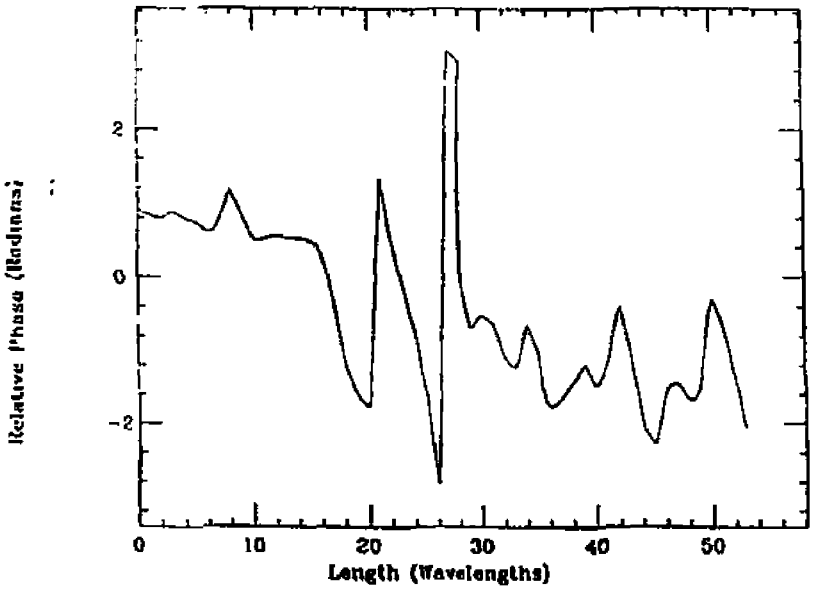

Figure 4d. Rate of power generation (MW per wavelength) versus distance.

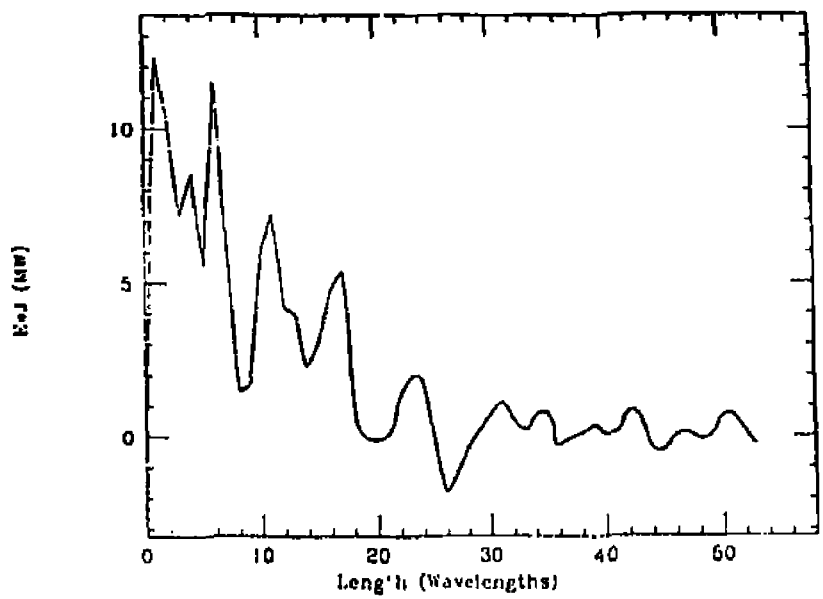

Figure 4e. Anode current versus distance.

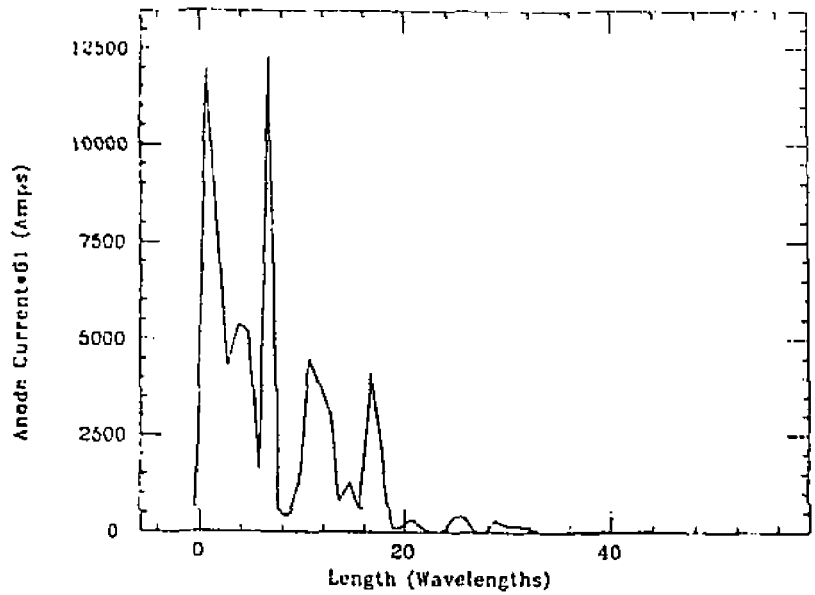

Figure 5. Fine resoltion plot of rate of power generation for typical calculation.

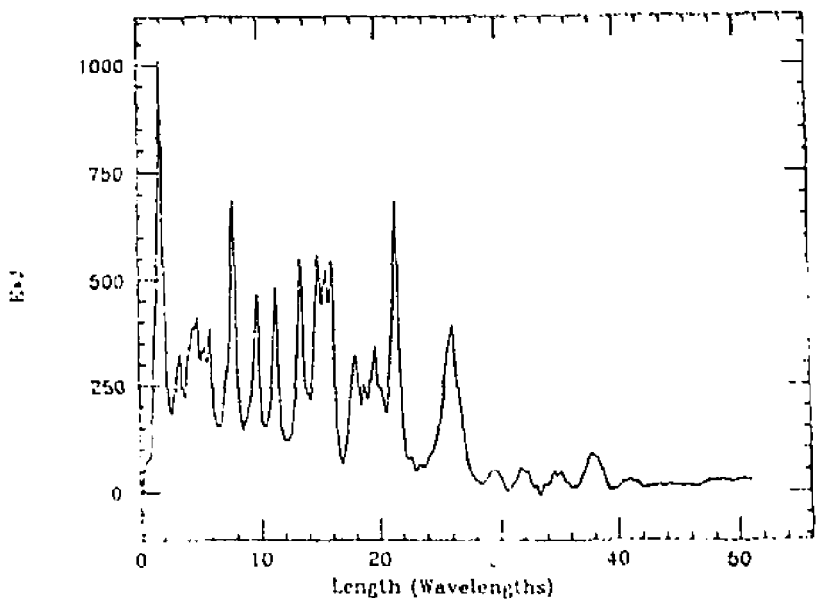

Figure 6a. Backward wave calculation with tapered impedance. BeO cathode, DC voltage 145 kV, 6 kGauss, .32 mm gap. Phase shift varied from 250 degrees per resonator at the output to 210 degrees at the input. Power level versus distance. The wavelength is the average value of 6.5 mm.

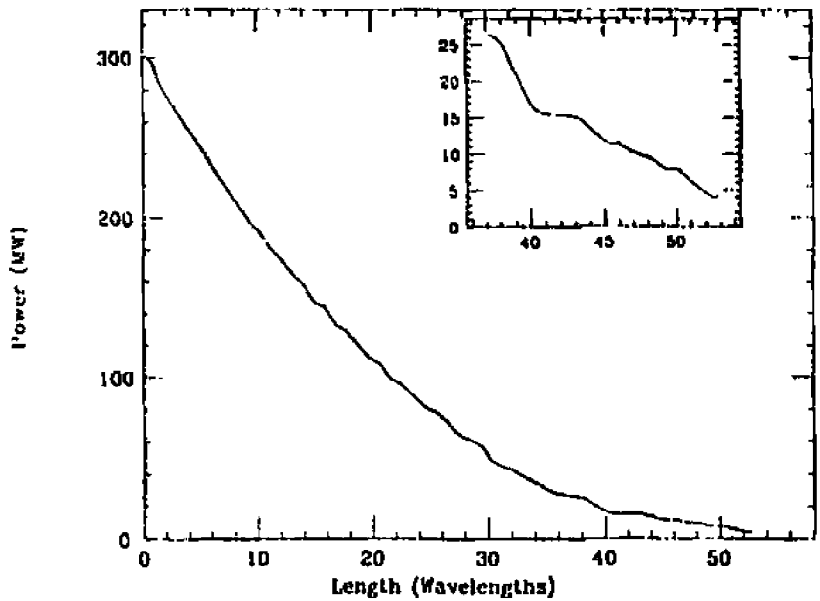

Figure 6b. RF phase versus distance.

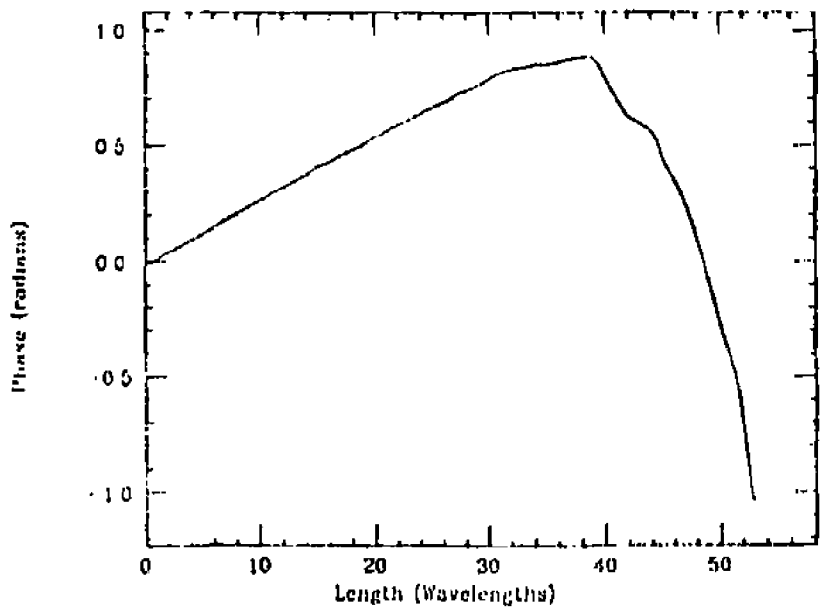

Figure 7. Simulation of output end of backward wave design. Electron position space distribution. The beam travels from left to right. Note the choke cavities which prevent RF from entering the drift space.

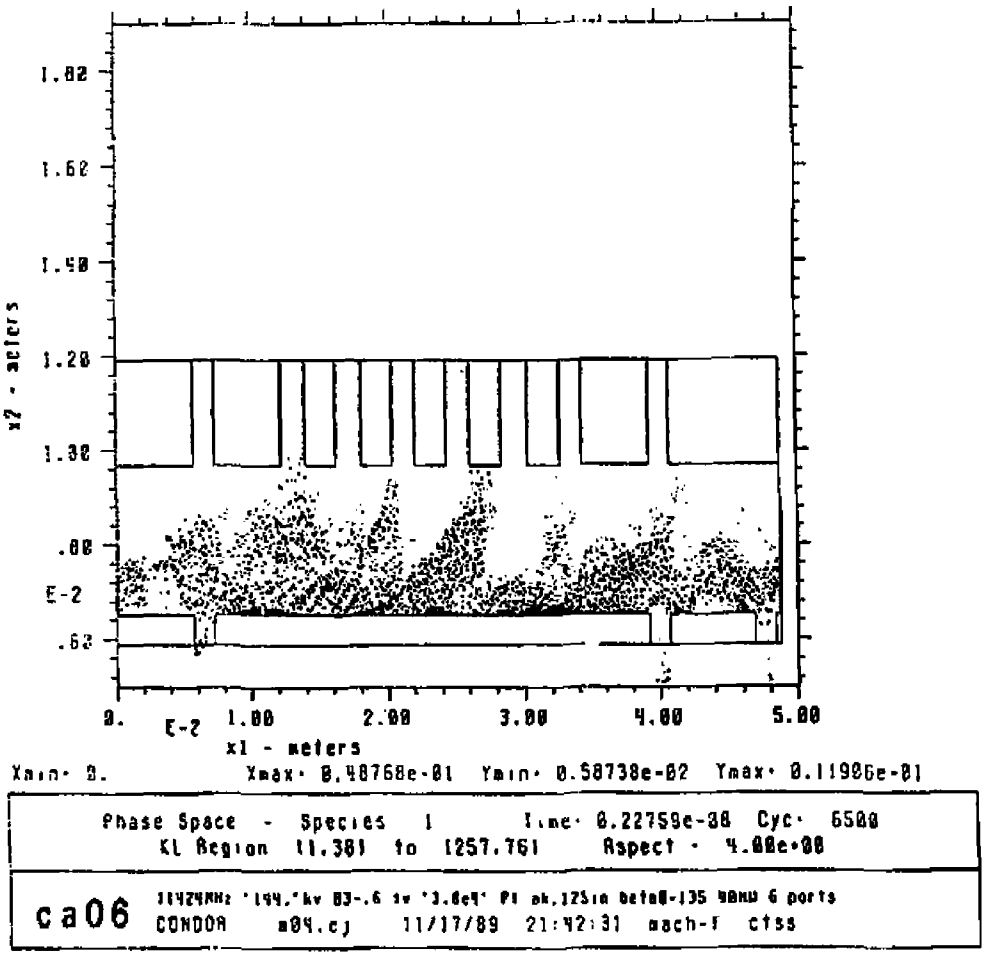

DISCLAIMER

Figure 8a. Forward wave simulation. Synchronous fundamental, 144 degree phase shift. BeO cathode, DC voltage 140 kV, 6 kGauss, .32 mm gap. Phase velocity was $7.74 \cdot 10^7$ m/sec. Power level versus distance. The wavelength is 6.8 mm.

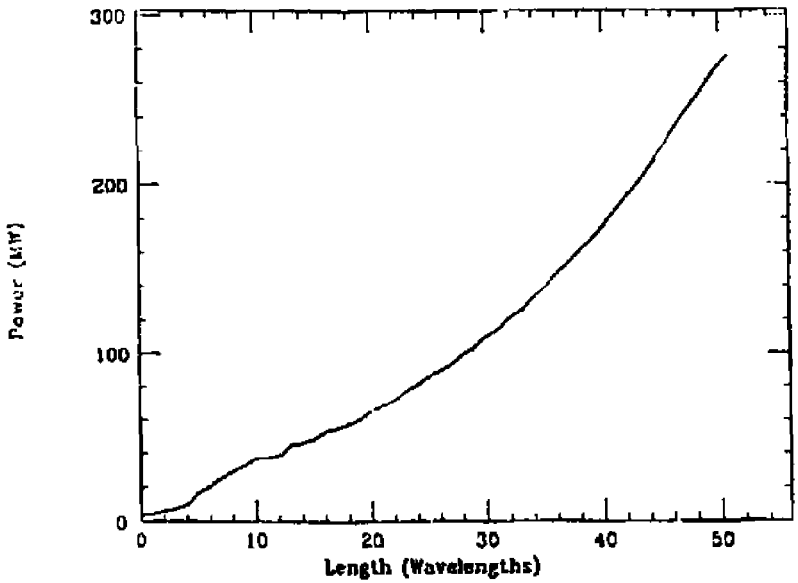

Figure 8b. RF phase versus distance.